

Porphyrin Supermolecules: Synthesis and Self-Assembly Features of Zinc-5-(3'-pyridyl)-10,15,20-tris(4'-hydroxyphenyl)porphyrin

Mikki Vinodu, Zafra Stein, and Israel Goldberg*

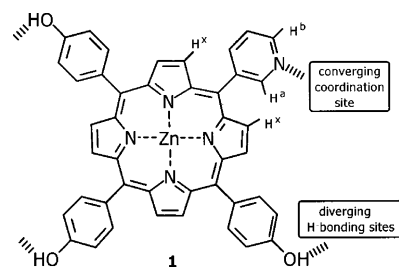
School of Chemistry, Sackler Faculty of Exact Sciences, Tel-Aviv University, 69978 Ramat-Aviv, Tel-Aviv, Israel

Received May 13, 2004

Targeted synthesis of the title compound, with one converging coordination site and three diverging H-bonding sites, has led to the formation of multiporphyrin oligomers by directed intermolecular coordination, without resorting to external auxiliaries. A uniquely structured cyclic tetraporphyrin supermolecule was detected in solution, isolated in the solid state, and characterized in detail by X-ray diffraction.

Several successful strategies for the designed construction of ordered multiporphyrin arrays by self-assembly have been developed in recent years, in a continuing effort to fabricate new supramolecular materials and devices for useful applications. This includes various solid-state formulations of extended multichromophoric arrays and zeolite-type architectures,^{1–3} as well as syntheses in solution of discrete cyclic and linear oligomeric systems by self-assembly.^{4–10} In the latter case, the cyclic tetrameric molecular boxes composed of various tetraarylmetal-porphyrins bearing the 4'-pyridyl function(s) deserved particular attention. These open molecular squares, cages, and capsules are sustained either by metal ion bridging auxiliaries (e.g., Pd, Pt, Ru, or Re)^{4–8} or by direct perpendicular intercoordination of the individual porphyrin units.^{11–13} In the present paper, we focus our attention on the formulation of discrete supramolecular

Chart 1



multiporphyrin aggregates directed by the convergent 3'-pyridyl function, and decorated by polar groups to allow their further self-organization into tertiary structures (e.g., on surfaces or in thin layers). The targeted synthesis of the 5-(3'-pyridyl)-10,15,20-tris(4'-hydroxyphenyl)porphyrin, and the isolation of its compact cyclic tetrameric entity with nano-sized dimensions and hydrophilic surface in the solid state, provides a suitable example to this end. It represents a scarce example of a cyclic 3'-pyridyl-substituted porphyrin oligomer formulated by direct coordination between the Zn-metalated porphyrin entities (**1**, Chart 1), without resorting to external auxiliaries.¹⁴ The different organization levels of this material in a condensed phase are characterized.

The design of discrete supramolecular clusters required an appropriate functionalization of the porphyrin scaffold. To ensure a convergent (rather than divergent) organization of several molecular units only a single 3'-pyridyl (basic) substituent was introduced onto the porphyrin framework, which was metalated with zinc ions having five-coordination (i.e., single axial ligand) preference. The remaining three *meso*-positions were substituted by the 4'-hydroxyphenyl

* To whom correspondence should be addressed. E-mail: goldberg@post.tau.ac.il.

- (1) Goldberg, I. *Chem. Eur. J.* **2000**, *6*, 3863–3870; *Cryst. Eng. Comm.* **2002**, *4*, 109–116.
- (2) Diskin-Posner, Y.; Dahal, S.; Goldberg, I. *Chem. Commun.* **2000**, 585–586; *Angew. Chem., Int. Ed.* **2000**, *39*, 1288–1291.
- (3) Kosal, M. E.; Chou, J.-H.; Wilson, S. R.; Suslick, K. S. *Nat. Mater.* **2002**, *1*, 118–121.
- (4) Fujita, N.; Biradha, K.; Fujita, M.; Sakamoto, S.; Yamaguchi, K. *Angew. Chem., Int. Ed.* **2001**, *40*, 1718–1721.
- (5) Iengo, E.; Zangrando, E.; Minatel, R.; Alessio, E. *J. Am. Chem. Soc.* **2002**, *124*, 1003–1013.
- (6) Dinolfo, P. H.; Hupp, J. T. *Chem. Mater.* **2001**, *13*, 3113–3125.
- (7) Drain, C. M.; Nifiatis, F.; Vasenko, A.; Batteas, J. *Angew. Chem., Int. Ed.* **1998**, *37*, 2344–2347.
- (8) Fan, J.; Whiteford, J. A.; Olenyuk, B.; Levin, M. D.; Stang, P. J.; Fleischer, E. B. *J. Am. Chem. Soc.* **1999**, *121*, 2741–2752.
- (9) Ogawa, K.; Zhang, T.; Yoshihara, K.; Kobuke, Y. *J. Am. Chem. Soc.* **2002**, *124*, 22–23.
- (10) Michelsen, U.; Hunter, C. A. *Angew. Chem., Int. Ed.* **2000**, *39*, 764–767.

- (11) Tsuda, A.; Nakamura, T.; Sakamoto, S.; Yamaguchi, K.; Osuka, A. *Angew. Chem., Int. Ed.* **2002**, *41*, 2817–2821.
- (12) Ikeda, C.; Hagahara, N.; Yoshioka, N.; Inoue, H. *New J. Chem.* **2000**, *24*, 897–902.
- (13) Fukushima, K.; Funatsu, K.; Ichimura, A.; Sasaki, Y.; Suzuki, M.; Fujihara, T.; Tsuge, K.; Imamura, T. *Inorg. Chem.* **2003**, *42*, 3187–3193.
- (14) While this work was in progress, similarly structured porphyrin tetramers were reported: (a) Balaban, T. S.; Goddard, R.; Linke-Schaetzl, M.; Lehn, J.-M. *J. Am. Chem. Soc.* **2003**, *125*, 4233–4239. (b) Tsuda, A.; Sakamoto, S.; Yamaguchi, K.; Aida, T. *J. Am. Chem. Soc.* **2003**, *125*, 15722–15723.

fragments to impart a hydrophilic character to the molecular surface of the assembling oligomer, thus further enhancing the convergent clustering of the porphyrin molecules. Stabilization of the oligomeric structure was anticipated also by probable interparticle hydrogen bonding. The free-base porphyrin was synthesized by reacting 0.075 mmol of 4-hydroxy-benzaldehyde with 0.025 mmol of 3-pyridine-carbox-aldehyde and 0.100 mmol of pyrrole in 350 mL of refluxing propionic acid. It was purified (as confirmed by TLC and proton NMR) by repeated column chromatography with eluents of varying polarity. Then, it was reacted with zinc acetate to yield the corresponding metalloporphyrin system **1**. Although **1** is soluble only in polar noninert solvents, which may act as competing coordinating ligands to the porphyrin core zinc ions, the UV-vis, ¹H NMR, and MS data of **1** confirmed its supramolecular nature.¹⁵

Thus, the UV-vis of **1** in pure methanol or methanol/dichloromethane mixture showed absorption peaks at 426 nm (Soret band) and 560 and 601 nm (Q-bands), which are independent of the solution concentration. Upon addition of a drop of pyridine, the Q-bands shifted to 566 and 606 nm (these bathochromic shifts in the Q-bands were observed even at low porphyrin concentration), indicating effective pyridine ligation to the metalloporphyrin and that the latter exists as a monomer in methanolic solutions. On the other hand, the UV-vis signals in acetone solution of **1** are concentration dependent. In dilute solutions (porphyrin concentration $< 1 \times 10^{-5}$ M), the absorption peaks appeared at 426, 560, and 601 nm, characteristic of monomeric entities. However, at increasing porphyrin concentrations a gradual red shift occurred in λ_{max} of the Q-bands, up to 563 and 606 nm at 1×10^{-4} M. It clearly suggests pyridyl-N to zinc coordination to yield self-assembled porphyrin tetramers.^{11,12} Supporting indications of the supramolecular aggregation are present in the NMR spectra (in acetone-*d*₆). The δ values of all the pyridyl protons were found to dramatically shift upfield, as reported earlier for the other Zn-porphyrin tetramers.^{11,12} Thus, comparison of the NMR data in acetone of the free-base porphyrin and **1** shows very large shifts of the pyridyl protons H^a and H^b from 9.39 to 2.14 ppm and from 9.04 to 1.70 ppm, respectively. The other pyridine proton signals exhibit smaller but significant downfield shifts from 8.61 to 6.90 ppm and from 7.83 to 6.10 ppm. The pyrrole protons appear perturbed by the self-assembly process as well. Their NMR signals change from a multiplet centered at 8.91 ppm in the free-base porphyrin to two separate sets, with intensity ratio of 3:1, at 8.95 ppm (multiplet) and 7.34

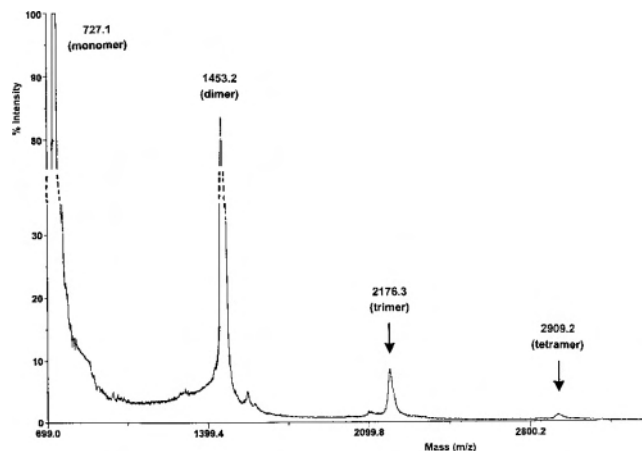


Figure 1. MS MALDI-TOF spectrum of **1**.

ppm (broad singlet) of the H^x protons. A considerably broader OH-proton signal in **1** (broad singlets at 7.60 and 6.90 ppm) than in the free-base porphyrin (well defined doublets at 8.07 and 7.30 ppm, respectively) may also result from higher aggregation mode of the porphyrin units in the former. On the other hand, the NMR analysis of **1** in DMSO-*d*₆ shows only negligible chemical shifts of the corresponding protons in relation to that of the free-base porphyrin, as DMSO is a strong coordinating solvent that prevents the porphyrin aggregation in solution.

The MS (MALDI-TOF) measurements of **1** (in 2-cyano-4-hydroxycinnamic acid matrix) provide further evidence for the supramolecular aggregation of the title compound in solution. The MS data show distinct peaks of decreasing intensity at positions corresponding to monomeric, dimeric, trimeric, as well as tetrameric porphyrin clusters (Figure 1). Qualitatively similar patterns were obtained in ESI-MS experiments. However, the presence of the bis- and trisporphyrin aggregates in **1** could not be confirmed independently by other means. The occurrence of the corresponding peaks in the MS spectra thus might have been effected by fragmentation of the tetrameric product (see below) by ionization excitation in these energized experiments.¹⁴

In view of these observations, and in order to isolate and characterize the most stable self-assembled product, we resorted to crystallization of **1** (from a nitrobenzene-methanol mixture by slow evaporation over a period of about 2–3 weeks), which afforded X-ray quality single crystals (**2**). The uniform constitution of **2** was confirmed by repeated measurements of the unit-cell dimensions from different single crystallites.¹⁶ Its structural analysis showed that the crystallization process afforded selectively the uniquely structured cyclic tetraporphyrin intercoordinated assembly. Solid **2** was obtained as octanitrobenzene solvate (as confirmed by thermogravimetric and diffraction analyses), and its molecular structure is illustrated in Figure 2.¹⁷

(15) Spectral data for the free-base porphyrin follow. UV-vis (CH₂Cl₂/MeOH): λ_{max} 420, 517, 556, 592, 650 (nm). ¹H NMR (acetone-*d*₆): δ 9.39 (d, *J* = 2.0, 1H), 9.04 (dd, *J* = 1.6, 1.6, 1H), 8.91 (m, 8H), 8.61 (m, 1H), 8.07 (d, *J* = 7.8, 6H), 7.83 (m, 1H), 7.30 (d, *J* = 8.4, 6H), and -2.89 (s, 2H); yield ~4%. Data for compound **1** follow. UV-vis (CH₂Cl₂/MeOH): λ_{max} 426, 560, 601 (nm). UV-vis (acetone 0.0001 M): λ_{max} 426, 563, 606 (nm). ¹H NMR (DMSO-*d*₆): δ 9.25 (d, *J* = 1.9, 1H), 8.92 (dd, *J* = 1.2, 1.3, 1H), 8.77 (m, 8H), 8.57 (m, 1H), 7.96 (d, *J* = 7.9, 6H), 7.85 (m, 1H), and 7.18 (d, *J* = 8.2, 6H). ¹H NMR (acetone-*d*₆): δ 8.95 (m, 6H), 7.60 (s br, 6H), 7.34 (s br, 2H), 6.90 (s br, 7H), 6.10 (s br, 1H), 2.14 (m, 1H), and 1.70 (m, 1H). MS(FAB): 726.1 (C₄₃H₂₇N₅O₃Zn). MS(MALDI): 727.1, 1453.2, 2176.3, and 2909.2, peaks that correspond to mono-, di-, tri-, and tetrameric porphyrin clusters, respectively.

(16) The low yields of the free-base porphyrin and **2** did not afford enough material for a reliable elemental analysis. A powder diffraction pattern from a bulk sample of **2** compared reasonably well with that calculated from the single-crystal structure, but its complexity (due to the very large unit cell) prevented an accurate analysis.

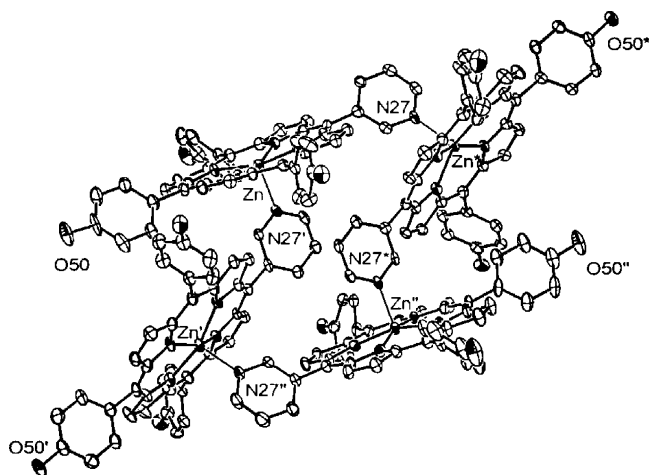


Figure 2. ORTEP representation of tetramer **2** (with 40% probability thermal displacement ellipsoids, excluding the nitrobenzene solvent of crystallization). The four Zn–N27 interporphyrin coordination bond distances are within 2.124–2.157(3) Å.

The crystallographic evaluation of **2**, a 280 non-hydrogen atom problem (along with the nitrobenzene solvent, some being severely disordered between different sites) presented a formidable challenge. It confirms the assembly of the metalloporphyrin species into (nearly centrosymmetric) cyclic tetramers by effective Zn–N(pyridyl) coordinations at 2.12–2.16 Å. The convergent organization of the porphyrin components is further stabilized by π – π interactions between the inward turning N27' and N27* pyridyl rings which partly overlap one another at an average distance of 3.51 Å. The van der Waals dimensions of the oval-shaped supermolecule (which represents a thermodynamically stable product)¹⁴ are 3.5, 2.1, and 1.6 nm, the latter referring to the distance between the roughly flat surfaces of the parallel porphyrin

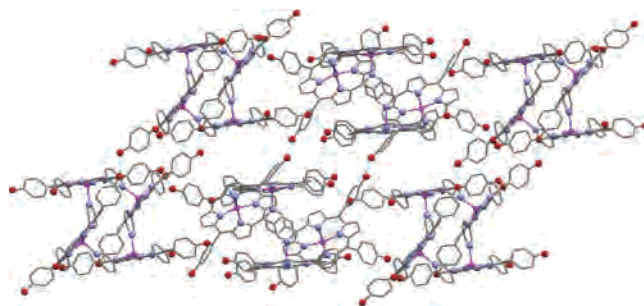


Figure 3. Section through the crystal structure of **2**, illustrating the accessibility of the peripheral hydroxyl groups for multiple hydrogen-bonding (dotted lines between neighboring tetramers).

components. Its other sides are lined with the OH-functions, which facilitate the formation of a stable crystal structure by enforcing, through an extended network of hydrogen bonds, the intermolecular organization (Figure 3). In the crystal, every molecule of **2** is involved in 11 OH...OH hydrogen bonds to the surrounding particles, all at O...O distances within 2.70–2.86 Å. The tetrameric species form a layered arrangement, the concave surfaces around the individual molecules along with the intermolecular voids being filled by the nitrobenzene solvent.

The potentially useful applications of cyclic supramolecular porphyrin assemblies, e.g., in catalysis as well as for guest-inclusion and transport, stimulate further design efforts of such materials.^{4,6,18} We have demonstrated here that a combined mechanism of programmed axial coordination and divergent hydrogen bonding provides a useful methodology for the supramolecular assembly of metallo-porphyrin entities into discrete supermolecules, and then tertiary self-organization of these “giant” species. Indeed, the secondary interactions were found to play an important organizing role not only in bulk solids,^{14a} but also in deposition of tetrameric porphyrin arrays on surfaces.¹⁹ This approach will be utilized in further studies, surveying the suitability of other metal ions of the porphyrin core, other ligating sites (e.g., various derivatives of pyridyl, imidazolyl, and quinolyl moieties), and alternative peripheral functions that can be used not only for interparticle self-organization but also as solubility controls and potential reactive sites.

Acknowledgment. This research was supported in part by The Israel Science Foundation (Grant No. 254/04).

Supporting Information Available: Crystallographic file in CIF format for **2**. This material is available free of charge via the Internet at <http://pubs.acs.org>.

IC049374+

(18) Keefe, M. H.; O'Donnell, J. L.; Bailey, R. C.; Nguyen, S. T.; Hupp, J. T. *Adv. Mater.* **2003**, *15*, 1936–1939.

(19) Milic, T.; Garino, J. C.; Batteas, J. D.; Smeureanu, G.; Drain, C. M. *Langmuir* **2004**, *20*, 3974–3983.

(17) Crystal data for $[4(C_{43}H_{27}N_5O_3Zn) \cdot 8(C_6H_5NO_2)]$: formula weight 3893.14, monoclinic, space group $P2_1/c$, $a = 24.3740(2)$ Å, $b = 29.0110(3)$ Å, $c = 31.4250(4)$ Å, $\beta = 93.6400(4)^\circ$, $V = 22176.2(4)$ Å³, $Z = 4$, $T = 110$ K, $D_{\text{calc}} = 1.166$ g·cm⁻³, 37399 unique reflections ($2\theta_{\text{max}} = 50.7$). Routine refinement of the solved structure converged only at $R1 = 0.135$ for 20432 reflections with $F > 4\sigma(F)$. Six molecules of the nitrobenzene solvent could be reliably included in structure-factor calculations. The two remaining solvent species, the overall location of which was clearly identified in difference Fourier maps, were found heavily disordered between four different sites around the unit cell origin, and their contribution was thus subtracted from the diffraction pattern by the “squeeze” method [Van der Sluis, P.; Spek, A. L. *Acta Crystallogr.* **1990**, *A46*, 194–201. Spek, A. L. *Acta Crystallogr.* **1990**, *A46*, C34.]. This refinement converged at final $R1 = 0.071$ for 20432 observations above the intensity threshold, $R1=0.115$ ($wR2 = 0.187$) for all 37399 unique data, $|\Delta\rho| \leq 0.60$ e/Å³. The integrated total residual electron density of the excluded solvent (497 electrons/cell) is consistent with additional two nitrobenzene species per asymmetric unit and with the results of thermogravimetric analysis. Supportive evidence for the occurrence of the cyclic tetramer was obtained from crystals prepared under slightly different conditions. They represent a pseudopolymorph of **2**, with lower content of the nitrobenzene solvent but much poorer diffraction quality and structure: [monoclinic, space group $C2/c$, $a = 25.132(1)$ Å, $b = 31.021(2)$ Å, $c = 23.351(1)$ Å, $\beta = 106.540(3)^\circ$, $V = 17452$ Å³, $Z = 4$].